Technical Program

ESM Today 2025

22nd Annual Student-Run Research Symposium
Department of Engineering Science and Mechanics

March 29th, 2025
Engineering Design and Innovation Building

University Park, Pennsylvania

Organized by:
Olivia Cook
Colin Williams
Jackson Schwarz
Nathan Leo
Asef Ishraq Sadaf

PennState College of Engineering

ENGINEERING SCIENCE AND MECHANICS

ESM Today Technical Program

March 29, 2025

Contents

Schedule of Events

Time	Activity	Location (EDI Building)
8:30 AM	Check-In and Refreshments	3rd Floor Common Area
9:00 AM	Welcome & Keynote Address	Room 325/326
10:00 AM	Break	
10:15 AM	Oral Presentations Session #1	Rooms 201, 202, 225, 226
11:15 AM	Break	
11:30 AM	Oral Presentation Session #2	Rooms 201, 202, 225, 226
12:30 PM	Lunch	3rd Floor Common Area
1:30 PM	Poster Session	Room 325/326
2:30 PM	Team Trivia	Room 325/326
3:15 PM	Awards, Wrap-Up, Pictures	Room 325/326

Keynote Address: Beyond Research - Applying the Scientific Method Throughout Your Life

Dr. Christine Masters

Speaker Biography: Dr. Christine Masters is currently the Assistant Dean for Academic Support and Global Programs in the College of Engineering at Penn State. She started her undergraduate degree as a 2+2 student at Penn State Erie, earning her bachelor's degree in mechanical engineering and her PhD in engineering science and mechanics, both from the Penn State College of Engineering. As a Teaching Professor of Engineering Science and Mechanics, Dean Masters has been a member of the Penn State faculty since 1997, has taught the subjects of Statics and Strength of Materials to thousands of Penn State students, supervised nearly 100 graduate teaching assistants, and served as the undergraduate coordinator for the engineering science honors program for 12 years before assuming her current role in 2014.
As Assistant Dean, she oversees academic advising, global engineering engagement, first year student engagement initiatives, and undergraduate records. She provides leadership to the college's academic integrity committee and has participated on several university-level initiatives and committees. Since becoming Assistant Dean, she has traveled to India, China, Peru, Italy, and Ireland in support of developing international opportunities for Penn State engineering students and had expanded the College's Global Engagement support from one part time staff member in 2014 to the current team of three full-time faculty and staff. She has enjoyed 37 years of marriage to Rob Masters, also a 2-time Penn State Engineering grad, and has spent most of her free time during those years watching their 4 children; Bart, Stephanie, Alek, and Sarah grow into amazing adults.

Oral Presentation Schedule

Time	Room 201	Room 202	Room 225	Room 226
10:15 AM	**Prabhav Borate**: Understanding shear failure through simultaneous synchrotron X-ray imaging and ultrasonic measurements	**Colin Williams**: A Transfer Learning Approach to Classify Additively Manufactured Ceramic Parts with Complex Geometries using their Resonant Ultrasonic Response	**Nathan Leo**: Exploring Machine Learning Applications for Statistical 3D Microstructure Reconstruction from Single 2D Material Slices	**Jackson A. Schwarz**: Interlaminar Shear Strength of Carbon/Epoxy Composites Containing Magnetically Aligned Nickel-Coated, Diazotized Carbon Nanotubes
10:30 AM	**Yuanxin Xiao**: Bio-Inspired Optimization of Spicule-Inspired Structures for Enhanced Mechanical Performance	**Cory Ly**: Mode II Interlaminar Fracture Toughness of Nanoparticle Toughened Carbon/Epoxy Laminates Manufactured by Resin Film Infusion	**Raghul Asokkumar**: Quantitative Assessment of the Role of Local and Neighborhood Features on the Grain-Scale Response of Inconel 718	**Mique Gonzales**: Designing shape memory alloys for additive manufacturing to leverage free recovery in a self-deploying radiator
10:45 AM	**Taufiq Hasan Aneem**: Biocompatible Dual-Crosslinked Hydrogels from Lung-derived Decellularized Extracellular Matrix	**Manik Kumar**: Enhancing Microstructure Prediction with Neural Network Surrogate Lattice Models	**Andrew Bozek**: Active Reverberation Cancellation to Reveal a Signal of Interest	**Mohammad Jannesari**: Poroelastic model for limit case: Formulation refinement and finite element implementation
11:00 AM	**Hermann Klinghammer**: Nonlinear elastic response of Westerly Granite	**Silas Wieland**: Acoustic Mapping of Cold Sintered ZnO: Optimizing Processing Parameters through Ultrasonic Nondestructive Testing	**Foster K. Feni**: Thermal-induced Transformation in LDED Additive Manufactured Ti-rich NiTi Shape Memory Alloy	**Michail Skiadopoulos**: Deep Ultrasonic Imaging of Porosity: Tomographic Image Reconstruction by Wave Physics-guided Deep Learning
Break				
11:30 AM	**MD Mashfiqur Rahman**: Characterizing The Complex Dielectric Properties Of Permafrost Across Freeze-Thaw Cycles	**Lei Ding**: In-situ vacancy mapping at nano-scale using 4DSTEM	**Yingxin Zhu**: Revealing the evolution of mechanical damage in large-scale 2D materials by in-situ electron microscopy	**Asef Ishraq Sadaf**: Synchrotron X-ray informed numerical simulation of wave propagation in fractured rock
11:45 AM	**Hamidreza Afzalimir**: Evaluating the effect of solute hydrogen atoms on the acoustic nonlinearity parameter of aluminum	**Marzia Momin**: 3D-printed flexible neural probes for recordings at single-neuron level	**Evan Bozek**: Characterizing the elastic response of fractured rock under stress using synchronous in-situ X-ray imaging and ultrasound	**Xinyu Wang**: The Effects of Gamma Irradiation of MOSFETs and Response to Electrical Stress
12:00 PM	**Lovejoy Mutswatiwa**: Grain structure and defects control by high-intensity ultrasound during direct energy deposition additive manufacturing of Al7075 alloy	**Ali Bastani Lay**: Detection and Localization of Acoustic Emission Events in a Lab-Scale Friction Experiment Using the STA/LTA Triggering Algorithm, the Akaike Information Criterion (AIC) and the Geiger's Method	**Feihong Liu**: Numerical and Analytical Modeling of Homogenized Wave Attenuation on Two-phase Microstructures	**Joseph Sgarrella**: Neural network controller algorithms for mimicking emergent dynamics of biological swarm
12:30 PM	**Jia-Yu Yang**: Water-Free Deep Eutectic Solvent Conductive Ionic Gel with Superior Mechanical Stability for Smart Biomedical Applications	**Maryam Ghodousi**: Development of Field Deployable Spray-On Array Transducers for High-Temperature Applications		

Poster Session

- **Characterizing The Complex Dielectric Properties Of Permafrost Across Freeze-Thaw Cycles** - MD Mashfiqur Rahman, Arafat Hossain, Steven Perini, Michael Lanagan
- **3D-printed flexible neural probes for recordings at single-neuron level** - Marzia Momin, Luyi Feng, Salahuddin Ahmed, Jiashu Ren, Arafat Hossain, Sulin Zhang, Tao Zhou
- **Characterization of Dielectric Materials Beyond Room Temperature Using the Lab-Developed Temperature Split Cavity (TSC) Method** - Arafat Hossain, Steven Perini, Michael Lanagan
- **Using Cognitive Load To Develop and Optimize Virtual Engineering Mechanics Learning Experiences Through an Eye Tracking-Based Framework** - JP Robbins, Judith A. Todd
- **Biocompatible Dual-Crosslinked Hydrogels from Lung-derived Decellularized Extracellular Matrix** - Taufiq Hasan Aneem, Joseph Christakiran Moses, Ibrahim Tarik Ozbolat
- **Retrieval of frictional parameters from continuous hybrid ultrasonic-acoustic monitoring using physics-informed neural network (PINN)** - Prabhav Borate, Jacques Rivière, Samson Marty, Chris Marone, Daniel Kifer, Parisa Shokouhi
- **High-Efficiency Phosphor Thin Films with Controlled Lateral Displacement for Low Color Crosstalk in Micro-LED Displays** - Zengzhi Pei, Justin Otto, Asim Mohammed A Noor Elahi, Jian Xu
- **Designing an Accessible 3D Model Viewing Platform and Models to Increase Students Spatial Understanding while Learning Engineering Subjects** - Micah A. Smith, Adomas Povilianskas
- **High-throughput In-Situ Ultrasonic Monitoring of Melt Pool Dynamics and Phase Transformations in Laser Additive Manufacturing** - Nathan J. Kizer, Jordan S. Lum, Rosa E. Morales, David M. Stobbe, Christopher M. Kube
- **Self-Assembly Enabled Printable Asymmetric Self-Insulated Stretchable Conductor for Human Interface** - Salahuddin Ahmed, Marzia Momin, Jiashu Ren, Hyunjin Lee, Tao Zhou
- **Architecting Periodic Columnar-Thin-Film Bilayer with a Central Layer Defect as Spectral Reflection-Hole Filter** - Abdul Rehman, Akhlesh Lakhtakia
- **An Adsorption Dominated Miniaturized Multifunctional Biosensor Based on In-situ Functionalized MXene and Laser Induced Graphene based Electrodes for Health Monitoring** - Abu Musa Abdullah, Md. Abu Sayeed Biswas, Ankan Dutta, Shuvendu Das, Xianzhe Zhang, Wanqing Zhang, Fatema Tuz Zohra, Arantza Moreno Calva, Huanyu Cheng
- **Microfabricated Mesh Depth Electrodes for Chronic EEG Monitoring in Mice** - Zein Chehab, Tao Zhou, Bruce J. Gluckman
- **Age-Specific Breast Cancer Modeling: Investigating Extracellular Vesicles via 3D Bioprinting** - Ilayda Namli, Ibrahim Tarik Ozbolat
- **Numerical Implementation of Incompressible Neo-Hookean Hyperelastic Model for Nonlinear isothermal Isotropic Elastic Material Behavior** - Dinesh Sharma, Dr. Francesco Costanzo

Art in Science Gallery

The ESM Today 2025 Art in Science competition showcases the beauty found in scientific research through compelling visual representations. These images highlight the intersection of science, art, and technology.

Click here to vote, or scan the QR code below!

Trapped Yet Free: Cell Navigation beyond Hydrogel Boundary

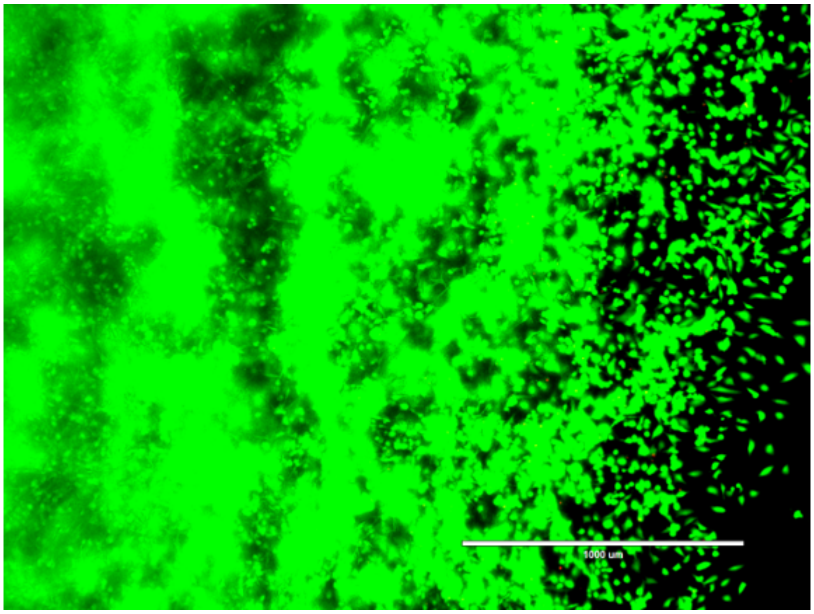

Taufiq Hasan Aneem, Joseph Christakiran Moses, Ibrahim Tarik Ozbolat
Description: Encapsulated within a photocrosslinked dECM hydrogel, cancer cells defy confinement, adapting and migrating beyond the gel's boundary. The balance between restriction and movement reveals the dynamic interaction between cells and their microenvironment.

Catastrophic Failure in a Rough Fracture Sample

Vertical Slice Horizontal Slice

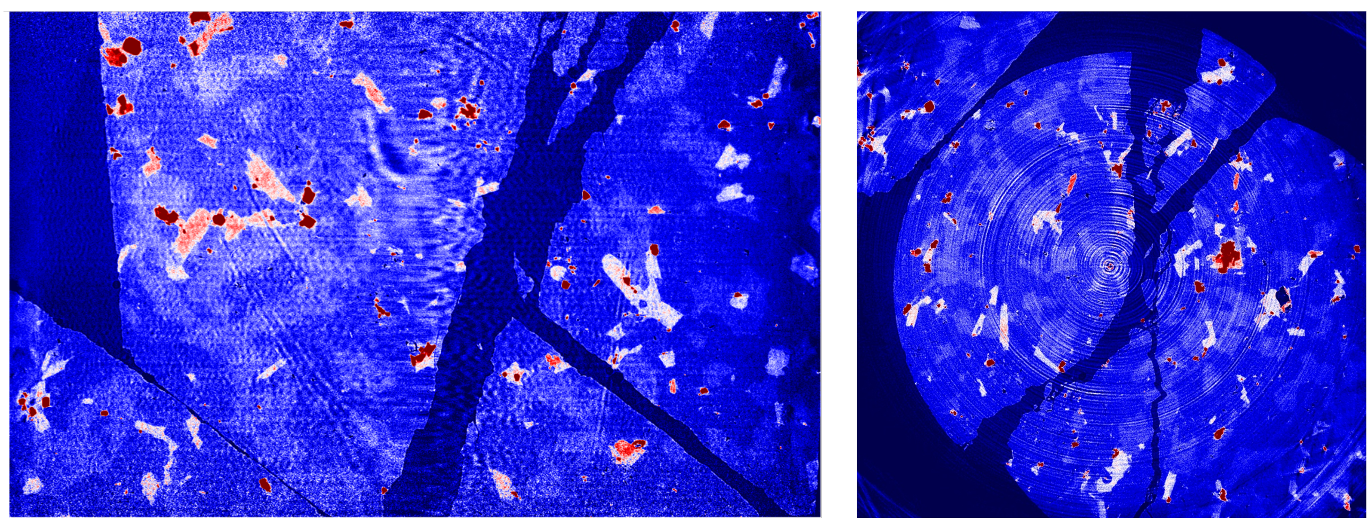

Prabhav Borate, Jacques Rivière, Parisa Shokouhi
Description: Synchrotron X-ray microtomography imaging of Westerly Granite sample fractured at $45°$ shows progressive damage accumulation, leading to catastrophic failure and a new secondary fracture.

The Cosmic Landscape of a Hair Follicle

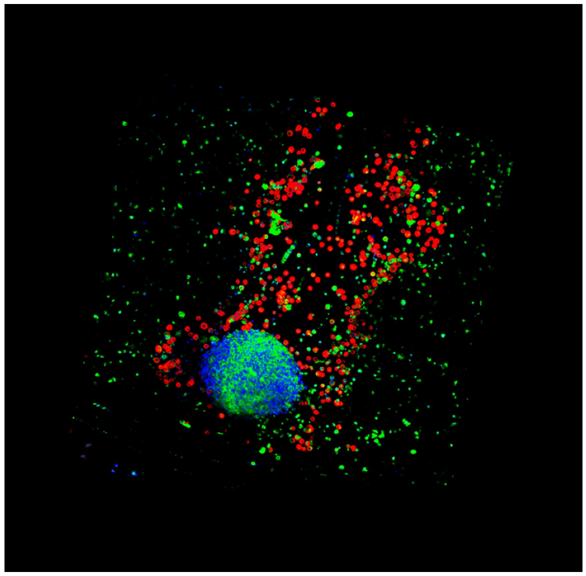

Irem Deniz Derman, Laura Garriga, Myoung Hwan Kim, Medine Dogan
Description: This image represents a fluorescence microscopy visualization of a human hair follicle, stained with K14 (Keratin 14) and AE15 markers, essential for understanding follicular structure and cellular organization. The K14 marker stains the basal layer of the outer root sheath (ORS), highlighting proliferative keratinocytes that contribute to follicular regeneration. The AE15 antibody specifically targets proteins within the inner root sheath (IRS), which supports proper hair shaft formation by aligning and hardening the keratinized cells.

Ettringite decomposition and cracks formation in concrete due to fire exposure

Massina Fengal, Erwann Rayssac
Description: Scanning electron micrograph of concrete after fire exposure, showing decomposed ettringite needles and crack formation in the Portland cement paste.

Inside Frozen Earth: Micro-CT Reveal of Permafrost Secrets

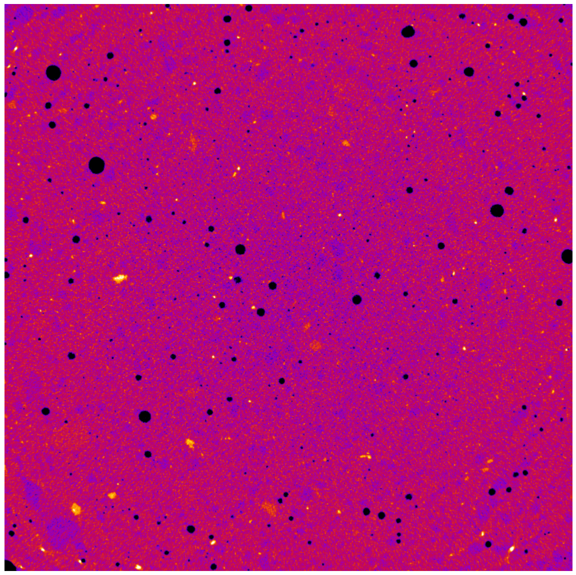

MD Mashfiqur Rahman, Michelle Quigley, Michael Lanagan

Description: At first glance, these images appear as abstract patterns of dark voids and dense formations, but to me, they tell a deeper story—one of a fragile, frozen landscape undergoing transformation. A permafrost sample composed of clay and water was scanned using micro-CT imaging at 20 µm resolution to analyze its internal structure and phase distribution. The high-resolution scan differentiates mineral grains, ice-filled pores, and water-rich regions, providing insights into porosity, water retention, and structural stability.

Total Focusing Method Ultrasonic Image

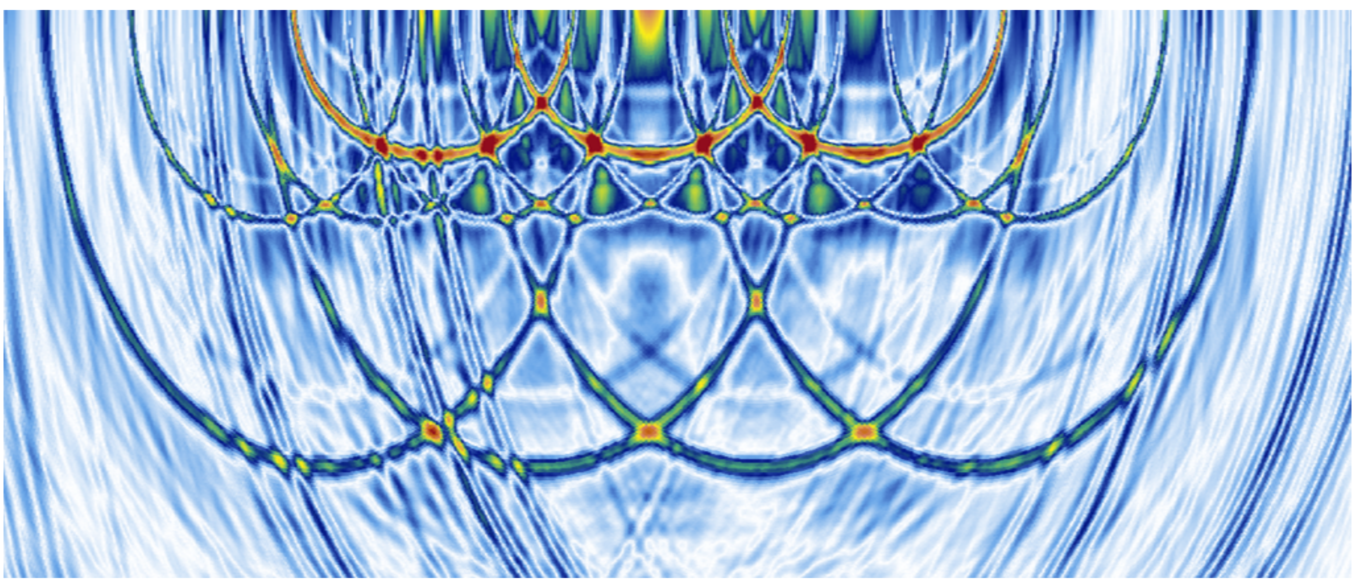

Maryam Ghodousi, Cliff J. Lissenden

Description: Illustration of TFM image captured from a high temperature spray-on phased array transducer for defect detection.

Abstracts

Room 201

Understanding shear failure through simultaneous synchrotron X-ray imaging and ultrasonic measurements

Prabhav Borate, Evan Bozek, Mark Rivers, Jacques Rivière, Parisa Shokouhi

Processes such as oil recovery and CO_2 sequestration can lead to earthquakes - a type of shear failure. This primarily occurs along pre-existing fractures when the applied shear stress surpasses the fracture's frictional strength. Shear failure is influenced by factors including fracture roughness, contact area, strength, and off-fault rock damage. In this study, we integrate in-situ time-lapse synchrotron X-ray imaging with ultrasonic probing to monitor laboratory shear failure events. Experiments are conducted using a custom-built triaxial loading apparatus that applies axial and confining pressure to pre-fractured cylindrical Westerly Granite samples. A pair of spring-loaded piezoelectric transducers is used to simultaneously track changes in elastodynamic properties and acoustic emission activity during shearing tests. Smooth and rough fracture samples are used to examine their impact on frictional behavior, elastodynamic properties, and acoustic emissions. The entire X-ray transparent pressure cell is mounted on a rotating stage in front of the synchrotron beam and high-resolution camera lens, enabling the recording of time-lapse 2D radiographs. These images provide insights into fracture and host rock deformation, contact evolution, and wear development at the interface. Additionally, pre- and post-shearing 3D X-ray computed tomography scans enable the changes in contact area and distribution to be measured. The elastodynamic and acoustic emission data will be analyzed alongside 2D and 3D imaging results to assess how fracture properties influence shear failure behavior. These findings will enhance our understanding of shear failure effects on strain distribution, acoustic emissions, and elastodynamic characteristics such as wave speed and amplitude in fractured rock.

Bio-Inspired Optimization of Spicule-Inspired Structures for Enhanced Mechanical Performance

Yuanxin Xiao, Niloofar Fani, Fariborz Tavangarian, Christian Peco

Bio-inspired structural optimization significantly advances materials engineering by mimicking nature's highly efficient designs. Spicule-inspired structures (SISs), modeled after Euplectella aspergillum, exhibit exceptional mechanical resilience due to their hierarchical organization. By integrating Finite Element Method (FEM) simulations with experimental validation, this study explores the influence of various structural parameters on mechanical performance. The investigation focuses on the effects of different numbers of layers, layer thickness ratios, variations in layers' Young's modulus, and the introduction of soft interfaces. Experimental validation, conducted through 3D-printed SIS prototypes and three-point bending tests, confirms the FEM predictions, highlighting the effectiveness of specific multilayer configurations in enhancing mechanical strength. Additionally, the study incorporates principles of nacre-like layered design to explore toughening mechanisms, improving fracture resistance and overall mechanical performance. A detailed examination of the cross-sectional and longitudinal morphology of spicules reveals the presence of interlocking organic layers that act as nanoscale adhesives, redistributing energy during deformation. To precisely model interlayer interactions, frictional contact mechanics and fracture mechanics are integrated. The resulting normal and tangential reaction force formulations are implemented into a cohesive zone model (CZM) within an optimized 3D SIS framework, aimed at reducing computational costs and modeling complexity. Furthermore, 3D-printed dog-bone specimens with varying interface geometries are fabricated to validate the CZM-based fracture mechanics predictions experimentally. This research provides a fundamental understanding of bioinspired toughening strategies, contributing to the development of next-generation SIS-based materials for biomedical implant applications.

Biocompatible Dual-Crosslinked Hydrogels from Lung-derived Decellularized Extracellular Matrix

Taufiq Hasan Aneem, Joseph Christakiran Moses, Ibrahim Tarik Ozbolat

Decellularization removes cellular components from native tissues while preserving the extracellular matrix (ECM) enriched with collagen, sulfated glycosaminoglycans (sGAG), elastin, and other proteins. Porcine lung tissues were decellularized using sodium dodecyl sulfate (SDS), Triton-X100, and alternating hypertonic/hypotonic sodium chloride (NaCl) solution. Efficacy of the processes was confirmed by DNA quantification and histological staining, demonstrating substantial removal of cellular debris. Although all approaches retained ECM components, SDS removed significantly more collagen and sGAG since it is a harsher treatment. All three types of decellularized ECMs (dECMs) were then used to form hydrogels via both thermal and photocrosslinking yielding dual-crosslinked scaffolds. Photocrosslinking occurred through the formation of dityrosine bonds under 460 nm light. A549 lung cancer cells were encapsulated in each hydrogel, and cell viability exceeded 95% across all samples for up to seven days. Optical imaging revealed that Triton- and hypertonic/hypotonic NaCl-treated dECM hydrogels facilitated cell migration beyond the scaffold, while the SDS-treated matrix provided a more compact structure that restricted movement. These findings indicate that while all dECM hydrogels remained highly biocompatible, SDS-based treatment produced a denser network that limited cell migration. Overall, these hydrogels exhibit strong potential for bioprinting and can be tailored for lung tissue engineering applications.

Nonlinear elastic response of Westerly Granite

Hermann Klinghammer, Parisa Shokouhi, Derek Elsworth, Jacques Rivière

The long-term goal of this work is to develop a nonlinear acoustic imaging method which can monitor the stress state in rocks, with applications to CO_2 sequestration, geothermal energy or oil/gas. To this end, we investigate the nonlinear elastic response of cylindrical samples of Westerly granite, either intact and transected perpendicular to the long-axis by a mated fracture, in a series of pump-probe experiments inside a modified triaxial cell that allows ultrasonic monitoring in transmission. The pump consists of axial and confining stress oscillations of amplitude 0.5 MPa and frequency $f0 \approx 8.3$ mHz to the quasi-static axial and confining stresses. Between two subsequent oscillations, the axial stress is varied stepwise upward and downward in the range [1 – 17] MPa, while the confining pressure is kept constant. The elastic state of the sample is probed by repeated transmission of 500-kHz pulses between the sample's end surfaces. Two

nonlinear elastic parameters are obtained from the measurements. The offset R0 captures the average change in wave velocity occurring during the oscillation, while R1 captures the amount of wave velocity change taking place at the pump frequency f_0. A positive (respectively negative) value of R0 is found when the quasi-static axial stress was previously increased (decreased). Surprisingly, R1 for the intact sample is larger than that of the fractured sample, even though the mated fracture represents an additional nonlinear interface in the system. Our results are discussed in light of two previous similar studies.

Characterizing The Complex Dielectric Properties Of Permafrost Across Freeze-Thaw Cycles

MD Mashfiqur Rahman, Arafat Hossain, Steven Perini, Michael Lanagan

Remote sensing in the Arctic regions is an essential tool for tracking the changing landscapes due to climate change, employing a wide range of frequencies in the electromagnetic spectrum to assess the condition of permafrost. Permafrost is a complex material of solid, liquid, gas, organic, and inorganic phases with each constituent contributing to the broadband dielectric response. In this study, permafrost was synthesized from sand, silt, and clay mixed with various amounts of water. Various weight fractions of permafrost/water mixtures were prepared by mixing sand, silt, and clay with different amounts of water. Microwave characterization and IR spectroscopy were subsequently performed on these mixtures to analyze their properties. The dielectric permittivity and loss of individual permafrost constituents in the dry and wet states were measured from radio frequency to infrared, using various reflection and transmission techniques. A coax reflection method was developed to provide complex dielectric data between 200 MHz and 26 GHz over a temperature range from 25 to -15 ℃. Dry constituents had low permittivity (ϵ_r<5) and low dielectric loss (tan$\delta < 0.02$). Wet constituents had high permittivity (10<ϵ_r<40) and there was a significant dielectric relaxation in the GHz frequency due to the dipolar state of water. Linking broadband dielectric and thermodynamic responses of water-organic and water-inorganic interfaces in permafrost will provide critical insight into the dipolar mechanisms governing permittivity and loss during the freeze-thaw cycle.

Evaluating the effect of solute hydrogen atoms on the acoustic nonlinearity parameter of aluminum

Hamidreza Afzalimir, Cliff Lissenden

Hydrogen embrittlement is a degradation mechanism that has gained recognition relatively recently and poses a significant threat to the structural integrity of engineering components exposed to hydrogen, such as storage systems and pipelines. Hydrogen atoms, due to their small size, can easily diffuse through these components and accumulate at interstitial sites and defects such as grain boundaries. This accumulation often leads to reduced ductility and a higher risk of brittle fracture. Nonlinear ultrasound, which is sensitive to material nonlinearity—closely linked to microstructural and atomistic defects—can be employed to detect hydrogen content in engineering components. We utilized atomistic scale simulations based on density functional theory to calculate both linear elastic constants (second order) and nonlinear elastic constants (third order), with and without solute hydrogen atoms. This approach helped assess how material nonlinearity and thus nonlinear ultrasound sensitivity are influenced by solute hydrogen. Our findings indicate that the impact of solute hydrogen on the acoustic nonlinearity parameter (ANP) varies based on the atom's location and the direction of wave propagation. Interestingly, in some cases, the presence of hydrogen decreased the ANP, contrary to simpler models at larger scales which suggest that any elastic inhomogeneity should increase ANP. Nevertheless, our results are consistent with experimental observations showing that ANP can decrease due to such inhomogeneities, attributed here to solute hydrogen atoms. We further explored the effects of solute hydrogen residing at grain boundaries with varying hydrogen concentrations. Our data revealed that ANP does not exhibit a consistent pattern with changes in hydrogen concentration and is also dependent on the direction of wave propagation. These insights significantly enhance our understanding of nonlinear ultrasound's capabilities to detect atomistic-scale defects, thereby improving diagnostic strategies in nondestructive evaluation.

Grain structure and defects control by high-intensity ultrasound during direct energy deposition additive manufacturing of Al7075 alloy

Lovejoy Mutswatiwa, Judith A. Todd, Edward W. Reutzel, Brady Sawyer, Cory D. Jamieson, Christopher M. Kube

Additive manufacturing (AM) offers advantages, including geometric flexibility and material grading capabilities over conventional fabrication techniques. However, the range of printable alloys is restricted due to solidification cracking, and intolerable microstructures. Ultrasonic melt processing presents a promising solution to refine grains and reduce defects without changing the alloy composition. This presentation will highlight how varying amplitudes and intensities impact grain refinement and solidification in ultrasonic vibration-assisted direct energy deposition (DED) AM of Al7075 and Scalmalloy. We custom-designed an Al7075 rectangular substrate, equipped with a high-power ultrasonic transducer, for installation in the DMG MORI LASERTEC65 Hybrid AM system. The substrate was engineered to excite the second transverse bending vibration mode at 19.3 kHz. Additionally, a high-speed camera captured melt pool surface dynamics with and without sonication. In this talk, we will connect the effects of ultrasound on melt pool dynamics with microstructural development, detailing the roles of acoustic cavitation and streaming.

Water-Free Deep Eutectic Solvent Conductive Ionic Gel with Superior Mechanical Stability for Smart Biomedical Applications

Jia-Yu Yang, Huanyu Cheng, Cheng-Hsin Chuang

Hydrogels offer excellent mechanical properties and biocompatibility, making them suitable for applications like wound dressings and electronic skin. However, their water content is sensitive to temperature changes, affecting long-term stability. This study replaces the water in hydrogels with deep eutectic solvent (DES) to create a water-free conductive ionic gel with superior mechanical properties (strain > 400%), stability (-80 to 70°C), and conductivity (4.83 mS/cm). These features enable its use in motion sensing, electro-stimulation wound dressings, and battlefield hemostasis, highlighting its potential for smart sensing and biomedical applications.

Room 202

A Transfer Learning Approach to Classify Additively Manufactured Ceramic Parts with Complex Geometries using their Resonant Ultrasonic Response

C. L. Williams, K. Shahed, G. Manogharan, M. H. Lear, and P. Shokouhi

As additive manufacturing (AM) becomes more industrially prevalent, developing rapid and nondestructive methods to inspect AM parts is growing in importance – especially for geometrically complex components. Here, resonant ultrasound spectroscopy (RUS) is coupled with finite element (FE) analysis simulations and supervised machine learning (ML) to classify AM ceramic samples with two different internal geometries. Variations in the frequency spectra of nominally similar samples make conventional RUS analysis techniques ineffective for classification (e.g., peak finding). It is hypothesized that these variations result from nonuniform shrinkage, which was observed across samples from X-ray computed tomography scans. Due to the limited size and complexity of the experimental dataset, a transfer-learning-based ML approach is utilized to improve classification accuracy. A dataset predominantly composed of synthetic resonance frequencies from high-fidelity FE simulations is used to train a Random Forest (RF) classifier for predictions on unseen experimental data. Results reveal the efficacy of including the synthetic data in training – an RF model trained on 50 simulated and 3 experimental frequency spectra has a testing accuracy that is 13.72% higher than a model trained on the same 3 experiments alone. Accuracies greater than 70% are achievable with training sets constituting less than 10% of the experimental data. This transfer-learning approach – where FE simulations constitute most of the training dataset while experimental data comprise the testing dataset – is shown here for the first time in RUS analysis. The results highlight the effectiveness of integrating physics-based simulations to enhance the classification of complex parts based on their RUS spectra.

Mode II Interlaminar Fracture Toughness of Nanoparticle Toughened Carbon/Epoxy Laminates Manufactured by Resin Film Infusion

Cory Ly, Dr. C.E. Bakis

One of the most common types of composites for structural applications is a laminated composite; a composite constructed from layers of fiber bonded together by a polymer matrix. One significant disadvantage of a composite laminate is its susceptibility to interlaminar fracturing, the cracking of the polymer matrix between the composite fiber layers. Therefore, one of the main areas for improvement is improving the interlaminar fracture toughness of a composite matrix. A composite matrix can be toughened to increase the matrix's ability to absorb energy and resist stress before fracturing. One of the most common and easiest ways to toughen a composite is the addition of nanoparticles to a composite's matrix. Nanosilica and core shell rubber are some of the nanoparticles that are added to toughen a composite matrix. While prior work has shown that nanoparticles in a matrix significantly affect the mass density, modulus, and Mode I fracture toughness of the matrix, the Mode II fracture toughness G_{IIc} for the commercial nanoparticle dispersed epoxies has yet to be determined. The objective of this experiment is to characterize and compare the G_{IIc} of a composite matrix with the NS and CSR nanoparticles. It is hypothesized that the nanoparticles increase the G_{IIc} of the composite by blunting or deviating the crack tip during Mode II loading. The ASTM D7905 standard test is performed on composites manufacture with CSR and NS nanoparticles to determine the G_{IIc}. The G_{IIc} of the NS and CSR specimens are compared to a neat epoxy specimen.

Enhancing Microstructure Prediction with Neural Network Surrogate Lattice Models

Manik Kumar, Christian Peco

Biological networks exhibit emergent behavior by dynamically adjusting their mechanical properties in response to stimuli, governed by discrete localized microscale interactions that collectively determine macroscale behavior. One approach to modeling these discrete interactions is Lattice Spring Modeling (LSM). While LSM effectively captures microscale mechanisms, it faces computational challenges when applied to complex, heterogeneous biological systems across scales and heterogeneity at the macroscale, posing a computational challenge in multiscale modeling. To address this, we present a multiscale framework integrating deep neural networks (DNNs), the finite element method (FEM), and an LSM-inspired microstructure representation. Our approach establishes a flexible lattice spring system to simulate interacting discrete units, rigorously linking them to macroscale FEM through a data-driven multiscale connection. A unified DNN replaces heuristic constitutive assumptions by directly learning stress-strain relationships from discrete lattice interactions across diverse particle arrangements. These include soft and hard inclusions, which are further combined to form a macroscopically homogeneous material, gradient-varying polycrystalline solid, and fully randomized configurations. This enables rapid predictions of tissue responses in heterogeneous environments. Our results demonstrate that the model accurately captures material responses across these spatially varying structures, highlighting its capability to resolve mechanical heterogeneity in biological tissues.

Acoustic Mapping of Cold Sintered ZnO: Optimizing Processing Parameters through Ultrasonic Nondestructive Testing

Silas Wieland, Sevag Momjian, Dr. Andrea P. Argüelles

The cold sintering process (CSP) is a low-temperature densification method for ceramics, metals, and composites. CSP enables densification at 70-500 ℃, more than halving standard firing temperatures which are generally greater than 1000 ℃. A transient liquid phase drives densification by facilitating mass transport that defines final density, microstructure, and bulk material properties. This study explores how transient phase composition and distribution affect longitudinal wave speed and attenuation characteristics of CSP ZnO. A 20 MHz single-element transducer in a water immersion pulse-echo system provides thickness-averaged spatial maps for samples with densities from approximately 90% to 98% of theoretical density. Comparisons with Hashin-Shtrikman bounds assess alignment between measured wave speeds, theoretical elastic moduli, and microstructural effects. By explicitly linking residual transient phase behavior to mechanical strength, the work aids efforts tuning CSP parameters. The findings encourage a reevaluation of acoustic methods for material characterization, positioning them as tools for optimization of processing conditions in ceramic fabrication. This work underscores the sensitivity of ultrasonic techniques to subtle microstructural variations, such as porosity and phase distribution, offering improved evaluation techniques for ceramic materials.

In-situ vacancy mapping at nano-scale using 4DSTEM

Lei Ding, Yang Yang

Vacancies are gaps where atoms are missing in a material's crystal lattice. These defects are small, often too tiny to detect with even the best microscopy technique, but they play a big role in materials. They impact materials' melting behavior, phase changes, and corrosion processes. To study these processes, we need to characterize vacancy behavior precicely. Current techniques for analyzing vacancies have strengths and weaknesses, yet they struggle to reveal details at the nanoscale and in-situ. This presentation introduces a method to in-situ map vacancies using Four-Dimensional Scanning Transmission Electron Microscopy (4D-STEM). 4D-STEM provides 4D structural data of the material. By pairing 4D-STEM with Density Functional Theory (DFT) simulations, vacancies in a NiCr alloy at the nanoscale was successfully mapped. Another example is from our recent research: characterizing vacancy distribution during CuZn corrosion in real time. Using MEMS in-situ heating chips with 4D-STEM and DFT, we tracked vacancy changes during a corrosion process in CuZn alloy called vacuum phase dealloying. Our work suggests how 4D-STEM can contribute to vacancy studies and aid in improving material development.

3D-printed flexible neural probes for recordings at single-neuron level

Marzia Momin, Luyi Feng, Salahuddin Ahmed, Jiashu Ren, Arafat Hossain, Sulin Zhang, Tao Zhou

Neural recording technologies offer valuable insights into neural activities that can help develop treatments for a wide range of conditions involving the brain, spinal cord, and other nervous systems. However, mismatches in material properties between these often-rigid electronic devices and biological neural tissues can lead to problems in biocompatibility (e.g., causing inflammation) and stability (e.g., dislocating contact). Here, we present a 3D-printable, flexible, stretchable electronic device with a porous, tissue-like structure designed for neural recording. This porous configuration bestows flexibility, stretchability, and conformability alongside chemical permeability, enabling integration with the brain and spinal cord. The 3D printability offers customization, cost efficiency, and scalability. The prototype device exhibits reduced impedance compared to conventional metal- or silicon-based devices, facilitating their precision in capturing neural activities at the cellular level in both the brain and spinal cord. The design lays a foundation for future research in brain-computer interfaces, neuromodulation, and neural prosthetics.

Detection and Localization of Acoustic Emission Events in a Lab-Scale Friction Experiment Using the STA/LTA Triggering Algorithm, the Akaike Information Criterion (AIC) and the Geiger's Method

Ali Bastani Lay, Parisa Shokouhi, Jacques Riviere

The detection and localization of acoustic emission (AE) or seismic events is essential across various scientific and engineering applications, from the health monitoring of structures to energy recovery (oil/gas, geothermal) and seismology. Among source localization methods, the Geiger's method remains one of the most widely used techniques for determining local earthquake hypocenters based on travel time differences. In this study, we extend this methodology to a laboratory-scale friction experiment which simulates earthquake nucleation processes. A single direct shear experiment was conducted using two blocks of Barre Gray Granite, during which AE sensors continuously recorded elastic wave emissions generated during shear. The raw AE signals were first bandpass filtered to remove noise and enhance signal quality. Subsequently, the short-time-average/long-time-average (STA/LTA) algorithm was first applied for event detection by identifying significant amplitude fluctuations indicative of AE events. Once detected, the Akaike Information Criterion (AIC) picker was utilized to determine precise arrival times for each event. The extracted arrival times across multiple sensors were then systematically associated and served as input to the Geiger algorithm, allowing for the three-dimensional localization of AE sources within the rock specimen. Challenges associated with manual thresholding, window sizes, as well as large differences in event sizes are discussed.

Development of Field Deployable Spray-On Array Ttransducers for High-Temperature Applications

Maryam Ghodousi, Cliff J. Lissenden

This study presents the development and testing of bismuth titanate (BIT) spray-on transducers, designed to operate reliably in high-temperature environments. Unlike traditional transducers that rely on couplants or bonding agents, which tend to degrade at high temperatures, the spray-on method applies a mixture of BIT, inorganic binder (Ceramabind 830), and water directly onto a substrate. This process creates a uniform, robust coating that remains stable at elevated temperatures, making it ideal for applications in harsh conditions. Twenty transducers were fabricated, and key properties such as thickness, d33 values, and resonance frequency were measured. Several of these transducers were subjected to thermal aging and thermal cycling to evaluate their durability in high-temperature conditions. The results demonstrated that the transducers remained functional, even after prolonged exposure to high temperatures, underscoring their reliability. In this ongoing work, transducers are arranged into phased arrays for Full Matrix Capture-Total Focusing Method (FMC-TFM) ultrasonic testing. These advanced techniques enable high-resolution ultrasonic imaging for nondestructive testing purposes. Supporting simulations were conducted in COMSOL to model the phased array configuration, while custom MATLAB code was developed to process the FMC data and produce TFM images. Overall, the findings demonstrate that the spray-on transducers can withstand thermal aging at 375 °C for one week, proving their potential for field-deployable applications in challenging environments where both stability and repeatability are critical.

Room 225

Exploring Machine Learning Applications for Statistical 3D Microstructure Reconstruction from Single 2D Material Slices

Nathan Leo, Christopher M. Kube

This research investigates diffusion-based deep learning approaches for reconstructing statistically representative 3D microstructures from single 2D material images. Unlike conventional methods requiring extensive 3D training data, our approach leverages denoising diffusion probabilistic models to generate complete 3D volumes while minimizing data requirements. The core methodology involves initializing a 3D volume with Gaussian noise and conditioning it with a real 2D microstructure slice that serves as a fixed reference. Through iterative denoising steps, the model gradually removes noise while propagating the structural characteristics of the conditioning slice throughout the volume. A key innovation is our "slicing operator" constraint, which forces partial 3D reconstructions to align with the input 2D data, ensuring statistical fidelity. Our approach should preserve both the dimensional statistics and orientation probabilities of the original material, with each grain maintaining consistent Euler angles throughout its volume. For grain materials, we track both single-point probability distributions (orientation probability at random points) and two-point distributions (probability of two points sharing the same grain at varying distances). Unlike GAN-based alternatives that face training instability, our purely diffusion-based solution offers a simplified pipeline with more stable convergence properties. The method should reconstruct various material types, including porous media, inclusion materials, spinodal decomposition structures, checkerboard materials, and fractal solids.

Quantitative Assessment of the Role of Local and Neighborhood Features on the Grain-Scale Response of Inconel 718

Raghul Asokkumar, Dhruv Anjaria, J.C. Stinville, Darren C. Pagan, Todd A. Palmer

Mechanical behavior of materials when loaded in extreme environments depend on their microstructure, loading conditions and the temperature. This microstructural contribution is a combined effect of the local microstructural features (grains and grain boundaries), the surrounding neighborhood and their interactions. Although, this effect of grain neighborhood on the mechanical properties is long accepted, quantitative assessment of these effects has proven challenging due to inherent limitations of traditional characterization methods. We present a multi-modal characterization approach combining electron backscatter diffraction (EBSD) and high-resolution digital image correlation (HR-DIC) to analyze the effects of neighborhood on strain distribution in grains in Inconel 718 alloy. Apart from the above-mentioned effects, to also account for the effect of precipitates, two samples were compared with and without excessive precipitation. Statistical analyses highlighted the effects of precipitation on deformation intensity and revealed quantitative correlations between local and neighborhood-based mechanical properties and strain distribution across grains in the small-strain regime.

Active Reverberation Cancellation to Reveal a Signal of Interest

Andrew Bozek, Dr. Cliff Lissenden, Dr. Bernhard Tittmann

A piezoelectric aluminum nitride (AlN) chip bonded to the outer surface of a metal fluid-containing structure can be used to ultrasonically inspect or test the structure and the wave path in the contained fluid in-situ. The material properties of AlN allow for the inspection in high temperature and/or high radiation environments. The propagation path of the ultrasonic wave considered for this presentation is in the pulse-echo mode through the bonded chip and metal, into a fluid, and finally reflected by some target in the fluid. This target can be a metal component submerged in the fluid, a liquid-gas boundary, or the other side of the metal structure (such as a pipe). The acoustic impedance mismatch between the metal surface and the fluid will cause a significant portion of energy to remain in the metal and generate echoes in the signal. These echoes can obscure the signals of interest returning from the target. By having the AlN chip generate a second pulse identical to the first pulse but delayed in time, the destructive interference of the two pulses can significantly reduce the amplitude of the echoes. In this presentation, a proof-of-concept active cancellation method for reducing coherent noise in the signal received by an AlN chip fixed to a metal plate is demonstrated at room temperature. A 10 dB reduction in the amplitude of the reverberations is observed, which is sufficient to provide a clear view of the signal of interest. Simple changes in the target were also investigated.

Thermal-induced Transformation in LDED Additive Manufactured Ti-rich NiTi Shape Memory Alloy

Foster K. Feni, Blake Miller, Reginald F. Hamilton

The functional properties of NiTi shape memory alloys (SMAs) involve the transformation of a high-temperature austenite phase to a low-temperature martensitic phase. The nucleation and growth of twinned martensite are highly sensitive to metallurgical factors such as composition and thermal history. Laser-directed energy deposition (LDED) additive manufacturing (AM) is emerging as a viable technology to produce functional SMA parts/components. However, the layer-wise deposition and spatially varying melt/solidification histories inherently introduce compositional and microstructural heterogeneity. For SMAs, spatial variations result in non-uniform functional properties in as-deposited near-net-shape parts/components. Designing NiTi-based alloys for LDED-AM has been explored for tuning composition and microstructure, and tailoring optimal shape memory properties and performance. Here we introduce a novel thermal analysis approach that studies a critical shape memory characteristic feature referred to as thermoelastic reversibility. Moreover, this study explores a novel Ti-rich NiTi alloy fabricated via LDED using elemental powder feedstock. Unlike equiatomic and Ni-rich NiTi alloys, Ti-rich compositions exhibit less sensitivity of transformation temperatures to composition and heat treatment. Thus, Ti-rich NiTi is expected to have a lower degree of spatial variation in properties. Differential scanning calorimetry (DSC) was employed to spatially characterize transformation temperatures of specimens sectioned at different locations within builds. Latent heat measurements from DSC analysis provided qualitative and quantitative measures to gain insights into the thermoelastic character. Results indicate minimal variation in transformation temperatures within a build. However, difference in thermoelastic character was observed between two studied orientations. This work provides key insights into the spatial uniformity and thermoelastic behavior of AM-fabricated Ti-rich NiTi SMAs.

Revealing the evolution of mechanical damage in large-scale 2D materials by in-situ electron microscopy

Yingxin Zhu, Ruyue Fang, Yang Yang

In the domain of intermetallic phase formation in the Al-Pt system, a multitude of research has been conducted. Our review aims to elucidate the intricate processes of precipitation and diffusion phenomena, emphasizing the role of Pt in the system. Historically, Al pillars, when subjected to elevated temperatures ranging from 300 °C to 400 °C, witnessed Pt diffusion into Al, leading to the formation of precipitates of assorted dimensions. While the presence of alumina on Al's surface modulates the precipitate shapes, the intriguing observation is the migration of these precipitates within the pillars, suggesting a deeper interplay between Pt precipitation and its concentration in Al. Crucially, extensive literature highlights the significant role of Pt in the Focused Ion Beam (FIB) preparation of Transmission Electron Microscope (TEM) samples. This review seeks to understand the underlying mechanisms of the Al-Pt system and to shed light on the broader implications of Pt in diverse material systems.

Characterizing the elastic response of fractured rock under stress using synchronous in-situ X-ray imaging and ultrasound

Evan Bozek, Prabhav Borate, Michail Skiadopoulos, Colin L. Williams, Chun Yu Ke, Clay Wood, Lalith Sai Srinivas Pillarisetti, Mark Rivers, Derek Elsworth, Jacques Rivière, Parisa Shokouhi

The elastic response of fractured rock is linked to the poromechanical properties of fracture networks, which is critical for monitoring geothermal energy reservoirs and CO_2 sequestration sites. For accurate remote assessment of sub-surface fracture networks under stress, it is necessary to improve quantitative relations between the seismic and morphological properties of fractures (i.e., contact area/distribution and fracture width). To accomplish this, we conduct laboratory-scale in-situ synchrotron X-ray imaging and through-transmission ultrasound on saw-cut rock samples under quasi-static and dynamic stress. 3D X-ray images are captured during quasi-static loading and unloading to estimate the aperture and contact area of the fracture as the stress changes. During dynamic stress oscillations, a series of 2D X-ray images are captured to measure displacement and strain distribution in real time. The ultrasonic signals during both quasi-static and dynamic loading are analyzed to understand how the amplitude, wave speed, and spectral content relate to the applied stress. These ultrasonic measurements are interpreted in terms of the changing state of the fracture as estimated from the X-ray images. Measurements are taken during both loading and unloading to capture hysteretic effects. In particular, we find connections between contact area and ultrasonic amplitude, between fracture aperture and ultrasonic spectral content, and between contact distribution and change in wave speed during dynamic stressing. These findings will improve the interpretability of seismic attributes to subsurface fracture properties.

Numerical and Analytical Modeling of Homogenized Wave Attenuation on Two-phase Microstructures

Feihong Liu, Andrea P. Argüelles, Christian Peco

This study presents a numerical and analytical study of wave attenuation in a two-phase matrix-inclusion microstructure. A numerical Green's function-based approach is developed for attenuation characterization, which avoids boundary enforcement in plane wave modeling. Analytical formulas based on the First-Order Smoothing Approximation (FOSA) are employed as a baseline for comparison. Assuming local isotropy, the effects of density and elasticity differences are examined, revealing good agreement between numerical and analytical predictions when only elasticity differences are present. However, FOSA overestimates attenuation when density differences are introduced, leading to a divergence in shorter wavelengths. This study presents the possibility of the proposed numerical method for wave attenuation analysis and exploring complex and multiphase microstructures. The observed discrepancies in density-related terms in FOSA highlight the need for further considerations in analytical modeling.

Room 226

Interlaminar Shear Strength of Carbon/Epoxy Composites Containing Magnetically Aligned Nickel-Coated, Diazotized Carbon Nanotubes

Jackson A. Schwarz, Ricardo Branco Nogueira Branco, Charles E. Bakis, Namiko Yamamoto

Carbon nanotubes (CNTs) have been shown to provide multifunctional reinforcement to carbon fiber reinforced polymers (CFRPs). However, obtaining well controlled properties through tight control of dispersion and orientation remains an ongoing challenge. Use of magnetic fields and magnetically responsive CNTs offer a potential solution to this challenge. In addition, surface functionalization of the nanoparticle surface can unlock further enhancements in mechanical properties. This investigation aims to develop a vacuum bag oven (VBO) resin film infusion (RFI) process in which CNTs of controlled distribution and orientation and epoxy are infused into dry carbon fabric. CNTs were fabricated with a thin coating of nickel for magnetic responsiveness and were functionalized using diazotization to improve dispersion and enable covalent CNT crosslinking within the epoxy matrix. A magnetic field was applied during CNT/epoxy film B-staging, laminate cure, or during both steps. Composite quality was assessed via optical microscopy; all the specimens had void contents below 1%. Their interlaminar shear strength (ILSS) was obtained using a short beam bending test. The baseline composite made with plain epoxy demonstrated the lowest ILSS, and total energy dissipated up to failure. Introducing 0.1% by volume randomly oriented CNTs provided modest increases to these quantities, and magnetic alignment of the CNTs provided further increases to these quantities. Ongoing efforts to scale up laminate production for interlaminar fracture toughness measurements will also be discussed.

Designing shape memory alloys for additive manufacturing to leverage free recovery in a self-deploying radiator

Mique Gonzales, Foster K. Feni, Reginald Hamilton, Damian Williams

Small satellites require small, lightweight, deployable thermal management systems. For this, deployable radiator fins are a sought-after technology for which shape memory alloys are investigated for their free recovery multifunctionality. NiTi-based shape memory alloys are the workhorse shape memory alloy system. In general, two classes of SMAs are well established: near-equiatomic/Ti-rich – for shape memory effect applications – and near-equiatomic/Ni-rich – for superelastic applications. The shape memory effect application gives rise to free recovery, and thus Ti-rich feedstock compositions are employed for Powder Bed Fusion (PBF) additive manufacturing in this work. The thermoelastic character of the material is assessed using multiscale thermomechanical testing and characterization using stress-strain and calorimetric analysis. Digital image correlation (DIC) is employed to probe varied length scales for characterizing multiscale reversibility of the evolving strain contours reflective of the transformation. Bending experimentation is investigated to evaluate candidate materials for their suitability in the end application. The thermoelastic character of the response is discussed in terms of key descriptors that are defined and identified from the bulk characterization. With this, we postulate the degree of potential for crystallographic reversibility of as-built and heat-treated materials.

Poroelastic model for limit case: Formulation refinement and finite element implementation

Mohammad Jannesari, Beatrice Ghitti, and Francesco Costanzo

Most formulations of poroelasticity lack the ability to address extreme conditions where all the fluid within the porous medium is expelled from some regions. In this study, we modify a poroelastic formulation based on mixture theory to represent the limit case where porosity approaches zero. We employ the MINI finite element to approximate solid displacement and develop an Arbitrary Lagrangian-Eulerian finite element model to solve for solid displacement, fluid velocity, and pressure. The model is verified using the method of manufactured solutions and applied to simulate a physical experiment in which porosity goes to zero.

Deep Ultrasonic Imaging of Porosity: Tomographic Image Reconstruction by Wave Physics-guided Deep Learning

Michail Skiadopoulos, Parisa Shokouhi

Deep learning (DL) models are increasingly leveraged to address the computational cost and resolution limitations of traditional ultrasonic imaging. Most conventional methods rely on full-matrix capture (FMC) data, where each phased array element sequentially acts as a source while all elements are receivers. Prior DL approaches are used for defect resolution in pre-generated images or to map FMC data to wave speed distributions, but they lack built-in physics constraints and increase computational cost, as the ground truth wave speed is extracted beforehand for model training. A promising alternative is full-waveform inversion via recurrent neural networks (RNNs), where wave physics is naturally encoded through sequential memory. Wave speed is treated as a trainable parameter, and the learned wave speed map is used to image defects. Backpropagation through time and automatic differentiation further accelerate parameter updates. However, prior studies have applied this concept only to guided wave testing. We propose an RNN-based full-waveform inversion framework for imaging subsurface pore defects by simultaneously reconstructing wave speed and viscous damping distributions from FMC data. The framework is tested on synthetic FMC data simulated for a square domain with a central circular defect (half-wavelength diameter). Instead of directly comparing recorded and predicted waveforms, the loss function is formed by applying the quadratic Wasserstein criterion to their probability density functions. Results demonstrate successful defect localization in wave speed and damping maps, though the defect shape is not fully recovered. Future work includes benchmarking against traditional imaging methods and extending to complex defect geometries and experimental data.

Synchrotron X-ray informed numerical simulation of wave propagation in fractured rock

Asef Ishraq Sadaf, Michail Skiadopoulos, Evan P Bozek, Derek Elsworth, Mark L Rivers, Jacques Rivière, Parisa Shokouhi

Seismic surveys are widely used to image underground, including reservoirs and fault zones. While seismic imaging effectively identifies fractures and fracture networks, its capability to characterize detailed fracture morphology remains limited. Since the aperture and connectivity of fractures significantly influence the fluid flow and mechanical properties of rocks, accurately quantifying these features from seismic data is crucial. We have developed methods to quantitatively relate seismic wave characteristics to the hydraulic and mechanical properties of fractures. Specifically, we have conducted experiments combining synchrotron X-ray computed tomography (CT) and ultrasonic through-transmission testing on a Berea sandstone sample containing a normal fracture under mechanical stress. X-ray CT scans provide detailed measurements of fracture aperture, true contact area, and contact size distributions as stress conditions are changed. Simultaneously, ultrasonic through-transmission testing provides measurements of wave speed, amplitude, and frequency content of the transmitted wave. Using the CT images, we have created detailed numerical models ("digital fractured rocks") that realistically capture the fracture under different stresses. Numerical simulations of ultrasonic wave propagation are performed using finite element modeling. Model parameters are calibrated by comparing numerical data to experimental ultrasonic measurements. Here, we present the development of our numerical models and comparisons between simulated and experimental ultrasonic data. These findings highlight a scalable approach to bridge laboratory-scale observations with field-scale seismic surveys.

The Effects of Gamma Irradiation of MOSFETs and Response to Electrical Stress

Xinyu Wang, Osama Awadelkarim

This study investigates the effects of gamma (γ) irradiation on the electrical stress response and thermal annealing behavior of silicon (Si) and silicon carbide (SiC) MOSFETs. Devices were irradiated with a Cobalt-60 (Co-60) source up to 2 Mega Rad, with terminals grounded or floating, followed by DC electrical stress and thermal annealing at 100 ℃. Results reveal that Si-MOSFETs exhibit significant threshold voltage (Vth) degradation due to radiation-induced charge trapping, which amplifies susceptibility to stress-induced damage. In contrast, SiC-MOSFETs exhibit superior radiation resilience but experience increased stress-induced charge trapping, particularly under negative bias. This degradation is attributed to the formation of nitrogen-related (N-related) defects, which arise from irradiation- and stress-induced bond breaking at passivated nitrogen sites near the interface. These defects contribute to subthreshold slope (SS) degradation, further affecting device reliability. Thermal annealing partially recovers Vth but fails to restore subthreshold slope (SS), indicating persistent interface charge trapping. These findings highlight the impact of irradiation under different bias conditions and emphasize the need for advanced defect passivation strategies to enhance the long-term reliability of MOSFETs in radiation-intensive environments.

Neural network controller algorithms for mimicking emergent dynamics of biological swarms

Joseph Sgarrella, Shishir Barai, Manik Kumar, William Laplante, Christian Peco

Collaborative swarm algorithms have drawn inspiration from biological swarms found in nature due to their coordination and optimization capabilities. Many current algorithms are developed in an ad hoc manner to capture the observed behavior of biological swarms, however, this approach is not able to systematically capture the emergent dynamics in advanced biological swarm organisms. In this work, inspired by a biological bottom-up approach, we aim to establish a decentralized controller algorithm rooted with a foundation of physical principles that capture the emergent dynamics of a biological swarm. We employ a strategy that enables the agents, which form the discrete body of the swarm, to mimic a unified continuum response observed in biological systems. Synthetic data from multi-agent simulations of well-known swarm algorithms will be leveraged to train neural networks to emulate swarm behaviors in response to internal and external stimuli. To assess the neural network's ability to capture the emergent behaviors, a campaign of simulations and physical experiments will be conducted with digital agents and physical robots. The flocking algorithm and ant colony algorithm have been chosen as benchmark tests to demonstrate the decentralized controller algorithm's ability to recreate the emergent dynamics of a biological swarm in a robotic swarm. The insights gained from these benchmarks opens a path to exploring the governing physical properties of more complex emergent systems, both discrete and continuous in nature.

Posters

Characterizing The Complex Dielectric Properties Of Permafrost Across Freeze-Thaw Cycles

MD Mashfiqur Rahman, Arafat Hossain, Steven Perini, Michael Lanagan

Remote sensing in the Arctic regions is an essential tool for tracking the changing landscapes due to climate change, employing a wide range of frequencies in the electromagnetic spectrum to assess the condition of permafrost. Permafrost is a complex material of solid, liquid, gas, organic, and inorganic phases with each constituent contributing to the broadband dielectric response. In this study, permafrost was synthesized from sand, silt, and clay mixed with various amounts of water. Various weight fractions of permafrost/water mixtures were prepared by mixing sand, silt, and clay with different amounts of water. Microwave characterization and IR spectroscopy were subsequently performed on these mixtures to analyze their properties. The dielectric permittivity and loss of individual permafrost constituents in the dry and wet states were measured from radio frequency to infrared, using various reflection and transmission techniques. A coax reflection method was developed to provide complex dielectric data between 200 MHz and 26 GHz over a temperature range from 25 to -15 ℃. Dry constituents had low permittivity (ϵ_r<5) and low dielectric loss (tan$\delta < 0.02$). Wet constituents had high permittivity (10<ϵ_r<40) and there was a significant dielectric relaxation in the GHz frequency due to the dipolar state of water. Linking broadband dielectric and thermodynamic responses of water-organic and water-inorganic interfaces in permafrost will provide critical insight into the dipolar mechanisms governing permittivity and loss during the freeze-thaw cycle.

3D-printed flexible neural probes for recordings at single-neuron level

Marzia Momin, Luyi Feng, Salahuddin Ahmed, Jiashu Ren, Arafat Hossain, Sulin Zhang, Tao Zhou

Neural recording technologies offer valuable insights into neural activities that can help develop treatments for a wide range of conditions involving the brain, spinal cord, and other nervous systems. However, mismatches in material properties between these often-rigid electronic devices and biological neural tissues can lead to problems in biocompatibility (e.g., causing inflammation) and stability (e.g., dislocating contact). Here, we present a 3D-printable, flexible, stretchable electronic device with a porous, tissue-like structure designed for neural recording. This porous configuration bestows flexibility, stretchability, and conformability alongside chemical permeability, enabling integration with the brain and spinal cord. The 3D printability offers customization, cost efficiency, and scalability. The prototype device exhibits reduced impedance compared to conventional metal- or silicon-based devices, facilitating their precision in capturing neural activities at the cellular level in both the brain and spinal cord. The design lays a foundation for future research in brain-computer interfaces, neuromodulation, and neural prosthetics.

Characterization of Dielectric Materials Beyond Room Temperature Using the Lab-Developed Temperature Split Cavity (TSC) Method

Arafat Hossain, Steven Perini, Michael Lanagan

The evolution of 5G telecommunications and the development of future 6G networks demand precise characterization of dielectric materials at high frequencies to enhance filter design and advanced electronic packaging. This paper evaluates essential dielectric parameters like relative permittivity, loss tangent, and temperature coefficient—within the 2–20 GHz range. Traditional measurement techniques, such as Split Post and Split Cavity methods, effectively assess small substrates like polymers, glasses, and ceramics at room temperature. To extend characterization beyond ambient conditions, this paper introduces the Temperature Split Cavity (TSC) and Temperature Coefficient of Capacitance (TCC) techniques, enabling measurements from –50 ℃ to 100 ℃ with a scale of 50 ℃ and –150 ℃ to 200 ℃, respectively. The TSC method revealed a linear relationship between relative permittivity and temperature, allowing accurate calculation of temperature coefficients. Validation against capacitor measurements at 1 MHz confirmed the consistency and reliability of TSC results. Additionally, the TSC technique successfully characterizes substrate materials with both ionic and covalent bonding. These findings demonstrate that TSC is a robust and reliable method for determining the temperature-dependent dielectric properties of materials essential for high-frequency telecommunications applications beyond room temperature.

Using Cognitive Load To Develop and Optimize Virtual Engineering Mechanics Learning Experiences Through an Eye Tracking-Based Framework

JP Robbins, Judith A. Todd

With the growing use of virtual reality (VR) in education and professional training, there is a strong demand to integrate it into undergraduate engineering curricula, especially for foundational courses like Statics and Strength of Materials. The ability to develop mental models to solve problems is a fundamental skill that students must develop in order to succeed not only in these courses, but throughout their engineering education and into their professional career. However, this is often a major challenge for students, especially when problems that require the student to think in three dimensions are accompanied only by two-dimensional figures. Cognitive Load Theory (CLT), which categorizes cognitive load into three types (intrinsic, extraneous, and germane), will be used as the theoretical framework. Unlike most similar studies, which treat cognitive load as a single variable, this project will use eye tracking to separately monitor these three load types and link them to specific eye movement patterns. Additionally, the project will investigate the impact of learner agency in VR experiences by developing three modalities of virtual lessons: a VR video, a guided VR experience, and an unguided, self-directed VR experience. Measuring each type of cognitive load independently through eye tracking will allow for real-time monitoring of students' cognitive states as they learn in a virtual environment. This work seeks to provide experimental evidence supporting the triarchic model of CLT and inform the design of VR learning environments for engineering education.

Biocompatible Dual-Crosslinked Hydrogels from Lung-derived Decellularized Extracellular Matrix

Taufiq Hasan Aneem, Joseph Christakiran Moses, Ibrahim Tarik Ozbolat

Decellularization removes cellular components from native tissues while preserving the extracellular matrix (ECM) enriched with collagen, sulfated glycosaminoglycans (sGAG), elastin, and other proteins. Porcine lung tissues were decellularized using sodium dodecyl sulfate (SDS), Triton-X100, and alternating hypertonic/hypotonic sodium chloride (NaCl) solution. Efficacy of the processes was confirmed by DNA quantification and histological staining, demonstrating substantial removal of cellular debris. Although all approaches retained ECM components, SDS removed significantly more collagen and sGAG since it is a harsher treatment. All three types of decellularized ECMs (dECMs) were then used to form hydrogels via both thermal and photocrosslinking yielding dual-crosslinked scaffolds. Photocrosslinking occurred through the formation of dityrosine bonds under 460 nm light. A549 lung cancer cells were encapsulated in each hydrogel, and cell viability exceeded 95% across all samples for up to seven days. Optical imaging revealed that Triton- and hypertonic/hypotonic NaCl-treated dECM hydrogels facilitated cell migration beyond the scaffold, while the SDS-treated matrix provided a more compact structure that restricted movement. These findings indicate that while all dECM hydrogels remained highly biocompatible, SDS-based treatment produced a denser network that limited cell migration. Overall, these hydrogels exhibit strong potential for bioprinting and can be tailored for lung tissue engineering applications.

Retrieval of frictional parameters from continuous hybrid ultrasonic-acoustic monitoring using physics-informed neural network (PINN)

Prabhav Borate, Jacques Rivière, Samson Marty, Chris Marone, Daniel Kifer, Parisa Shokouhi

Recent advancements in machine learning and deep learning have been utilized to predict laboratory earthquake events, a type of shear failure, from stick-slip friction experiments. These models estimate the timing and magnitude of shear failures by using features derived from ultrasonic or acoustic emission (AE) signals. This study integrates acoustic and ultrasonic data from shear experiments to develop physics-informed neural network (PINN) models. These models incorporate the Rate and State Friction (RSF) law, which is commonly employed to model fault frictional behavior, and the AE rate generation equation as physics-based constraints. The PINN framework enables direct estimation of RSF parameters from stick-slip friction experiments, eliminating the need for traditional velocity step experiments. Transfer learning (TL) PINN models are created by initially pre-training on data collected at a specific normal stress level. They are then used to predict shear failures and extract RSF parameters at different stress levels (with varying recurrence intervals) after being retrained with a limited set of new data. Results show that TL PINN models exhibit better performance in predicting shear failures and estimating RSF parameters under different stress conditions. Both standalone and TL PINN models demonstrate strong agreement between estimated and actual RSF parameters, validating that RSF parameters can be effectively inferred from laboratory stick-slip experiments using acoustic-ultrasonic data.

High-Efficiency Phosphor Thin Films with Controlled Lateral Displacement for Low Color Crosstalk in Micro-LED Displays

Zengzhi Pei, Justin Otto, Asim Mohammed A Noor Elahi, Jian Xu

In this study, an optimized nano-phosphor thin film was developed for Micro-LED applications, demonstrating high efficiency in color conversion and effective suppression of lateral photon displacement. The primary goal was to reduce color crosstalk, achieving a balance between absorption and transmission to support full-color Micro-LED displays, particularly in medium- to low-resolution applications. Experimental results validated the model's accuracy, with controlled lateral displacement closely matching the simulation predictions. The film exhibited a broad emission spectrum with CIE color coordinates near the D65 white point, confirming its potential for stable and high-quality color output. Additionally, the film maintained strong fluorescence intensity at elevated temperatures, showcasing superior thermal stability over traditional quantum dot materials. This study provides a practical approach to designing high-performance phosphor films, with future work focusing on optimizing optical properties to enhance Micro-LED display technologies.

Designing an Accessible 3D Model Viewing Platform and Models to Increase Students Spatial Understanding while Learning Engineering Subjects

Micah A. Smith, Adomas Povilianskas

3D vector mathematics is a crucial part of the engineering curriculum, and yet the tools and methods used to teach the subject matter do not reflect the best teaching practices. The purpose of this research is to develop new tools that improve students' understanding and comprehension. The study is in its first stage, which is to test a simplified 3D viewing platform with students where 20-40 engineering students complete a four-question assessment with either a 3D model or a 2D image of a mathematics problem spanning three dimensions. The effectiveness of these tools will be measured by using cognitive load theory and performing statistical analysis on the obtained data sets. Future phases of the project will include improving the viewport and conducting in class studies. The research aims to uncover whether these viewports improve students' understanding and visualization of 3D mathematics.

High-throughput In-Situ Ultrasonic Monitoring of Melt Pool Dynamics and Phase Transformations in Laser Additive Manufacturing

Nathan J. Kizer, Jordan S. Lum, Rosa E. Morales, David M. Stobbe, Christopher M. Kube

In-situ characterization of phase transformations during laser-based additive manufacturing (AM) offers crucial insights into material properties. While traditional monitoring relies on limited-access synchrotron X-ray facilities, this work presents a high-throughput ultrasonic characterization system as an accessible alternative for monitoring phase transformations and solidification in powder bed fusion processes. Multiple materials demonstrate the system's capabilities: Ti5553 and AlSi10Mg establish correlations between melt pool characteristics and solidification behavior, while Ti-6Al-4V and functionally graded SS304L-Ni20Cr illustrate solid-state phase transformations across varying compositions and processing conditions. The technique employs strategically placed focused immersion transducers to characterize grain formation and phase evolution during and after solidification. By leveraging ultrasound scattering within the partially solidified "mushy zone" between the solid substrate and liquefied melt pool, the system enables real-time tracking of critical solidification parameters. This ultrasonic monitoring approach maintains the spatial and temporal resolution necessary for detailed microstructural analysis while providing insights across systematic variations in laser power and scanning speed. By correlating transition region behavior with phase transformations and melt pool stability, this work establishes ultrasonic characterization as a robust, nondestructive tool for rapidly understanding process-structure relationships in AM processes.

Self-Assembly Enabled Printable Asymmetric Self-Insulated Stretchable Conductor for Human Interface

Salahuddin Ahmed, Marzia Momin, Jiashu Ren, Hyunjin Lee, Tao Zhou

Soft and stretchable conductors with high electrical conductivity and tissue-like mechanical properties are crucial for both on-skin and implantable electronic devices. Liquid metal-based conductors hold great promise due to their metallic conductivity and minimal stiffness. However, the surface oxidation of liquid metal particles in polymeric matrices poses a challenge in forming a continuous pathway for highly conductive elastic composites. Here, it is reported a printable composite material based on liquid metal and conducting polymer that undergoes a self-assembly process, achieving high conductivity (2089 S cm^{-1}) in the bottom surface while maintaining an insulated top surface, high stretchability (>800%), and a modulus akin to human skin tissue. This material is further applied to fabricate skin-interfaced strain sensors and electromyogram sensors through 3D printing.

Architecting Periodic Columnar-Thin-Film Bilayer with a Central Layer Defect as Spectral Reflection-Hole Filter

Abdul Rehman, Akhlesh Lakhtakia

Periodic bilayers of columnar thin films with central layer defects were fabricated and optically characterized. Experimental analysis indicates that an optimal number of unit cells will deliver the best performance as a spectral reflection-hole filter.

An Adsorption Dominated Miniaturized Multifunctional Biosensor Based on In-situ Functionalized MXene and Laser Induced Graphene based Electrodes for Health Monitoring

Abu Musa Abdullah, Md. Abu Sayeed Biswas, Ankan Dutta, Shuvendu Das, Xianzhe Zhang, Wanqing Zhang, Fatema Tuz Zohra, Arantza Moreno Calva, Huanyu Cheng

The advancement of multifunctional wearable, flexible, and stretchable sensors plays a crucial role in precisely monitoring human health biomarkers. However, high-performing sensors require highly sensitive, stable, and miniaturized electrodes. In this study, we introduced an in-situ Functionalized Ti-MXene and Laser-Induced Graphene (LIG) composite (FMLIG) electrode-based biosensor for monitoring body glucose using human sweats. The two-step direct laser printing contributed to the surface reduction of MXene onto LIG electrodes, which shifted the electrochemical reaction from diffusion-controlled to adsorption-controlled. The shift has been confirmed through both simulative and experimental approaches. The FMLIG electrochemical sensor exhibits exceptional glucose sensitivity of 2751.3 µA/mM.cm^2 with a miniaturized electrode area of 0.0079 cm^2 and a low limit of detection of 0.3 µM for sweat detection, along with excellent stability maintaining over 90.53% sensitivity for 21 days in ambient conditions. Furthermore, the sensor demonstrates high consistency in body glucose measurement across multiple human subjects. The miniaturized electrodes can further be implemented to fabricate highly sensitive multi-functional biosensor for space-constraint areas. The miniaturized size of the sensor enables seamless integration with VR-integrated health monitoring systems. Moreover, the FMLIG electrodes, when utilized as a humidity sensor, showcase impressive performance with high sensitivity of 20197.01 pF/RH, low response time of 27.57 s, and a rapid recovery time of 3.18 s. Additionally, the FMLIG composite electrodes exhibit remarkable capabilities in capturing skeletal muscle movements during grasping, with an observed increase in EMG amplitude by 167% compared to pristine LIG electrodes, even in the presence of sensible sweat, while maintaining an excellent signal-to-noise ratio. The sensors were further integrated with a VR mask to monitor physical and mental health. These devices show promising possibilities in health monitoring during VR mask usage

---

Microfabricated Mesh Depth Electrodes for Chronic EEG Monitoring in Mice

Zein Chehab, Tao Zhou, Bruce J. Gluckman

Electrocorticography (EEG) depth electrodes are essential tools for monitoring neural activity in mice, but current fabrication methods rely on labor-intensive manual assembly of gold wires within micron-scale tubes. To address this challenge, we present a novel mesh micro-implant featuring three electrodes spaced 100 µm apart along the x-axis, designed for improved scalability and handling. The device integrates a robust SU-8 backbone with gold tracks and SIROF-coated electrodes, which may be electrochemically activated in situ to enhance performance. A secondary SU-8 encapsulation layer ensures structural integrity, while a 20 µm thick PMMA layer enhances mechanical stability. The implantable section supports bio-absorbable silk coating on the electrode regions, providing temporary stiffness for implantation. A polyimide backing is incorporated for additional mechanical reinforcement. The I/O section includes three 1 mm connector pads, designed to accommodate rivet-based attachment, ensuring durability during implantation and external interfacing. Fabrication is performed in a cleanroom environment, leveraging multilayer photolithography and etching techniques to achieve precise electrode geometries. This approach eliminates the need for tedious manual assembly while ensuring reproducibility and high-throughput manufacturing. By offering a flexible yet structurally sound alternative to existing depth electrodes, this micro-implant has the potential to streamline chronic EEG recordings in small animal models, enhancing both usability and data reliability.

Age-Specific Breast Cancer Modeling: Investigating Extracellular Vesicles via 3D Bioprinting

Ilayda Namli, Ibrahim Tarik Ozbolat

Extracellular vesicles (EVs) are crucial mediators of intercellular communication in cancer progression, typically isolated from blood or plasma. However, in this study, we present a novel approach by generating organoids from patient-derived breast cancer cells and isolating EVs directly from these uniform, bioprinted organoid cultures. Using 3D bioprinting, we precisely control cell seeding, ensuring identical cell numbers and uniform organoid formation within a hydrogel matrix. This controlled environment allows us to investigate EV differences between young and elderly breast cancer patients under equal experimental conditions. Following EV isolation, we analyze their impact on MDA-MB-231 breast cancer cells and NHLF (Normal Human Lung Fibroblasts) to evaluate age-related variations in EV-mediated signaling. By comparing EV profiles between young and elderly patient-derived organoids and assessing their functional effects on recipient cells, our study provides insights into how aging influences tumor microenvironment interactions. This standardized bioprinting-based model offers a reproducible and physiologically relevant platform for studying breast cancer progression, addressing limitations in high-throughput techniques for age-specific cancer modeling. Our findings highlight the potential of bioprinted organoid-derived EVs as biomarkers and therapeutic targets, advancing personalized approaches in breast cancer research.

Numerical Implementation of Incompressible Neo-Hookean Hyperelastic Model for Nonlinear Isothermal Isotropic Elastic Material Behavior

Dinesh Sharma, Dr. Francesco Costanzo

Hyperelastic materials, such as rubber-like polymers and biological tissues (e.g., arterial vessels and blood clots), exhibit a nonlinear stress-strain relationship and can undergo large deformations while retaining their shape within the elastic region. Accurately modeling their behavior is critical for applications in engineering and biomedical fields, including vascular mechanics and soft tissue analysis. This study aims to numerically implement and validate an incompressible Neo-Hookean hyperelastic model to predict the mechanical behavior of such materials under large deformations. The model is implemented in MATLAB using Voigt notation and properties of symmetric tensors to optimize computational efficiency. Dual programs are being developed to compute the Second Piola-Kirchhoff Stress Tensor and the 4th-order Elastic Moduli Tensor. Strain energy is represented in terms of both principal invariants and principal stretches to ensure comprehensive validation. Preliminary implementation has achieved a reduction in computational complexity. Validation of the dual programs is currently in progress, with the goal of comparing numerical results against analytical solutions to ensure accuracy and robustness. Once validated, the developed algorithms will provide a reliable tool for simulating such materials, with potential applications in vascular mechanics and soft tissue analysis. The codes can also be integrated into finite element analysis (FEA) commercial software like COMSOL, enabling accurate predictions of nonlinear material behavior in engineering and biomedical applications.
